Spectroscopic Behavior of Composite, Black Thermal Paint, Solar Cell, and Multi-layered Insulation Materials in a GEO Simulated Environment

Jacqueline A. Reyes[(1)], Ryan C. Hoffmann[(2)], Daniel P. Engelhart[(3)], Heather M. Cowardin[(4)], Darren Cone[(5)]

[(1)] University of Texas at El Paso – Jacobs JETS Contract, 500 W. University Ave., El Paso, TX, 79968, USA, jareyes10@miners.utep.edu
[(2)] Air Force Research Laboratory, Space Vehicles directorate, Kirtland AFB, Albuquerque, NM, 87117, USA
[(3)] Assurance Technology Corporation, 84 South Street, Carlisle, MA, 01741, USA
[(4)] Jacobs, NASA Johnson Space Center, Houston, TX, 77058, USA
[(5)] University of Texas at El Paso – CASSMAR, 500 W. University Ave., El Paso, TX, 79968, USA

ABSTRACT

Materials currently populating Earth orbital regimes can be distinguished by comparing remote observational data to that of optical material measurements obtained in the laboratory. Experimentation for this research primarily involved the acquisition of spectroscopic measurements on materials of interest to the telescopic observational community for enhanced space situational awareness. Common spacecraft materials worthy of preeminent analysis for this investigation include a carbon-carbon (c-c) matrix composite, various black thermal paints, a GPS solar cell and three different cover glass components. These materials were subjected to a simulated geosynchronous Earth orbit (GEO) space environment with the intent of observing material optical property behavior over quantitative exposure time. The aforementioned materials have been measured in their pristine and GEO simulated exposed conditions. A reflectance spectrometer and a bi-directional reflectance distribution function (BRDF) optical system have been operated to perform material characterization, optical property analysis, and to further compare such data to telescopic observational data acquired on equal materials.

1 INTRODUCTION

Numerous spacecraft and rocket bodies have been launched and positioned within near Earth orbit since the first satellite, Sputnik, launched on October 4, 1957 [1]. As space missions are continuously implemented, the population numbers of objects in Earth orbit are expected to increase. There are ~17,000 (+5,000) objects tracked daily by the U.S. Strategic Command and ~70 new launches are executed each year [2]. These objects are faced with potential collision, explosion, or degradation events when remaining in orbit for extended periods. These events lead to the generation of orbital debris. As of April 1, 2019, of the 19,404 total objects cataloged by the U.S. Space Surveillance Network, 4,972 of them are payloads and a dominating 14,432 of the objects are rocket bodies and debris [3]. It is imperative that remote observations be performed on all articles in orbit to improve space situational awareness.

The following paper presents reflectance spectroscopic measurements and bidirectional reflectance distribution function (BRDF) evaluations taken on common spacecraft materials, some of which are likely candidates in the orbital debris population. The research goal is to assess optical properties of common spacecraft materials in their pristine conditions, as well as after environmental exposure using a space environmental chamber to simulate space weathering. The materials of interest include various black thermal paints, a Global Positioning System (GPS) solar cell, CMG, CMO, and CMX cover glasses, a c-c composite, and the multi-layered insulation (MLI) component Kapton®. These materials will prove that they have excellent properties in resisting the effects of damage that are common in both low Earth orbit and geosynchronous Earth orbit (GEO) based on the research discussed in this work.

1.1 Environment

Objects located in near Earth orbital regimes are surrounded by a plasma environment consisting of photons, ions, and electrons, as well as atomic oxygen and ultraviolet radiation, in vacuum conditions [4, 5]. In geosynchronous Earth orbit, the particles responsible for the most destructive effects on a material are electrons [5]. In order to mimic the GEO space environment, it was significant to ensure that high-energy electrons were present within a vacuum environmental chamber while having the spectral reflectance of the material surfaces measured to observe any optical property variations for this study.

Reflectance spectroscopy has assisted in providing material characterization dating back to the 1970's when asteroid examinations were conducted using its methods, and furthermore in the 1990's when its application expanded into characterizing orbiting spacecraft materials [6]. Secondly, knowing an object's position in orbit allows for better laboratory characterization in reference to illumination conditions and reflectance properties dependent on an object's aspect angle and general material properties. This can be addressed by evaluating the bi-directional reflectance distribution function (BRDF) of a material that can further relate to its albedo and size. Having knowledge of an object's material, size, and shape from examination in a laboratory setting, then can be used to improve size assessments of objects when employing remote optical measurements [7]. Reflectance spectroscopy has proven to function as an efficient apparatus having provided detailed characterization data from materials common in space design such as aluminum, pigmented paints, stainless steels, and various solar cells [8]. Spectroscopic data collected on materials in the laboratory serve as a reference for comparison with orbiting object spectroscopic or photometric data acquired remotely from telescopic systems.

2 INSTRUMENTATION

Optical reflectance measurements were performed on all material sample surfaces using a Spectral Evolution SR-3501 spectroradiometer having a range of 280-2500 nm. The SR-3501 utilizes a silicon photodiode array detector and two indium gallium arsenide photodiode detectors to read out the reflectance from 2,221 channels in 1 nm increments [9]. It has a spectral resolution of 4 nm between 280-1000 nm wavelengths, 5 nm at 1500 nm wavelength, and 7 nm at 2100 nm wavelength [9]. The illumination source used in coalition with the spectrometer was an Ocean Optics HL-2000-HAS halogen lamp, which delivered light between a 400-2100 nm range. The spectrometer and the lamp were used in conjunction with an integrating sphere to provide a hemispherical reflectance (HR) within the 280-2500 nm range. BRDF measurements were produced from a Light Tec Mini-Diff optical system device that operated using a 632 nm collimated light source. The Mini-Diff produced reflectance data from illumination impinging at 0°, 20°, 40°, and 60° angles of incidence on a target material surface.

Selected material samples for this study were subjected to simulated GEO conditions within the JUMBO Environmental Chamber at the Spacecraft Charging and Instrumentation Calibration Laboratory at Kirtland Air Force Base. The JUMBO chamber allowed for the materials to sit in vacuum and undergo electron radiation at a high energy of 100 keV generated from a Kimball Physics EG8105-UD electron gun. Vacuum levels are achieved in this system using mechanical, turbo, and cryogenic pumps.

Prior to weathering, each material had its initial HR and BRDF measured. Material samples were placed on a circular plate referred to as a carousel because this plate rotated in the chamber when undergoing electron exposure to ensure uniform irradiation occurred for all mounted samples. A Faraday cup was placed at the centermost point of the sample carousel to measure the electron flux for further determination of the fluence near the material sample locations within the chamber.

Throughout the space weathering operation, a HR measurement of all samples on the carousel was taken approximately every 2 hours. To execute this, the reflectance spectrometer's fiber optic cable was fed through a port on the integrating sphere and the illumination source was fed through a port adjacent to that of the fiber optic. The integrating sphere had an ~0.8 inch diameter opening to view the material sample surface. When taking a measurement, the integrating sphere would move to sit first over a Spectralon, followed by an Acktar black material. These two surfaces were necessary for instrument calibration purposes. The integrating sphere would then move to position itself over the first material sample on the carousel, and the carousel would rotate counter-clockwise to allow measurements to be taken on all mounted samples.

The set of materials selected for weathering was divided into two groupings to be taken during two different measurement campaigns. The reason was to keep samples of similar thickness grouped together to avoid various thicknesses of neighboring material samples to interfere with the integrating sphere. It was imperative to position the sphere flat against each material surface for accurate measurement acquisition. Therefore, although there were 12 sample slots on the carousel, only a few selected slots were occupied by material samples in a manner that best fit with each respective measurement campaign. The arrangement of materials mounted for testing are depicted in Fig. 1 and a list of the specific materials in their designated slot positions is outlined in Tab. 1.

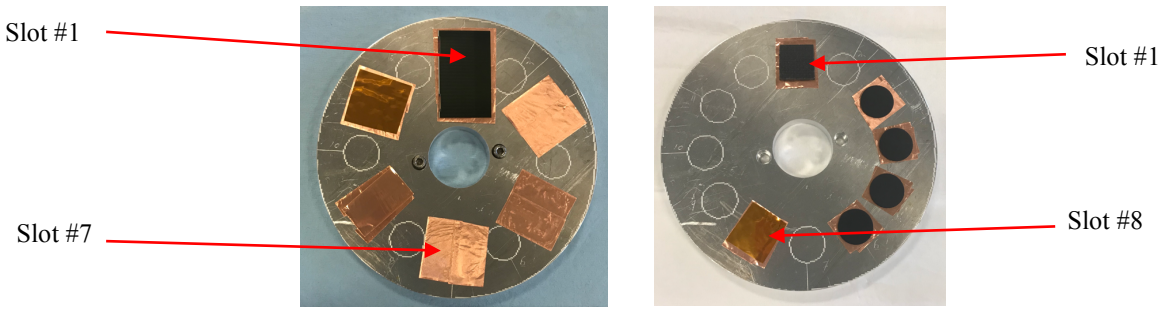

Fig. 1. Image of the sample carousel with materials mounted for (a) Campaign #1 and (b) Campaign #2.

Table 1. List of materials and their respective slot positions on the sample carousel for Campaigns #1 and #2.

CAMPAIGN #1		CAMPAIGN #2	
Slot #	**Material Sample**	**Slot #**	**Material Sample**
1	GPS Solar Cell (bare/without interconnects)	**1**	C-C Composite
3	CMG Cover Glass	**3**	Black Paint RM-550
5	CMO Cover Glass	**4**	Black Paint AZ-1000-ECB
7	CMX Cover Glass	**5**	Black Paint MLS-85-SB-C
9	Cu Tape	**6**	Black Paint MLS-85-SB
11	Kapton (aluminized)	**8**	Kapton (aluminized)

The spectrometer, through use of the integrating sphere, was able to provide HR measurements for all material surfaces throughout the space weathering experiment. The percent HR was calculated using the equation:

$$\% \text{ HR} = \frac{N_{sample} - N_{Acktar}}{\frac{N_{Spectralon} - N_{Acktar}}{R_{Spectralon}}} * 100 \quad (1)$$

where N represents the raw digital numbers provided by the spectrometer and $R_{Spectralon}$ refers to the calibrated reflection values that the Spectralon material possesses at a given wavelength. This calculation was executed for every material tested within the 280-2500 nm wavelength range and produced the percent HR curve for each sample.

3 MATERIALS INVESTIGATED

Materials widely and often used to compose spacecraft and rocket body structures had their reflectance measured spectroscopically for comparison with data of materials in orbit taken remotely. The materials selected for space-weathering lab simulations in this work included a bare GPS solar cell; CMG, CMO, and CMX cover glass sheets manufactured by Qioptiq; a c-c composite, RM-550 black paint, AZ-1000-ECB black paint, MLS-85-SB-C black paint, MLS-85-SB black paint; and aluminized Kapton. GPS solar cells are often silicon based with highly absorbing material properties. The bare cells were protected with a sheet of cover glass. CMG, CMO, and CMX cover glasses are thin, transparent, and brittle materials. They are cerium doped to protect solar cells from the harmful ultra-violet, proton, and electron radiation that exists in space conditions [10].

Carbon-carbon composites are constructed of numerous carbon fibers that are oriented in a multi-directional lay-up to achieve isotropic material properties. They have high fracture toughness, high thermal conductivity, a low coefficient of thermal expansion, and a high strength-to-weight ratio [11], making them ideal material candidates for space design. Black paints RM-550, AZ-1000-ECB, MLS-85-SB-C, and MLS-85-SB, provided by AZ Technology, are all thermally conductive and maintain their optical properties when in space domain [12]. RM-550 and AZ-1000-ECB are inorganic while MLS-85-SB-C is organic, and MLS-85-SB-C is an electrically conductive version of MLS-85-SB [12].

Kapton has had its optical properties measured in previous electron radiation studies [13, 14] but was still included in the two measurement campaigns involved in this study as a reference to ensure that the GEO simulated weathering was successfully produced within the chamber. Kapton is a thermoset polyimide film that has excellent chemical resistance, can withstand low and elevated temperature conditions, and does not melt [15]. These material properties are reasons why the polyimide film is incorporated in multi-layered insulation (MLI) materials used on a majority of space hardware components that are currently in orbit or will be launched in the future. Copper (Cu) tape was included as a material worth measuring during Campaign #1 since double-sided Cu tape was used to adhere the cover glass samples to the sample carousel and therefore was analyzed to compare the transparent qualities of the various cover glasses. The Cu tape measured was single-sided to avoid adhesive interference with the cyclic movement of the integrating sphere against the tape sample. The tape served for coverglass color feature analysis.

4 RESULTS & ANALYSIS

All materials were subjected to examinations that simulated space weather in the JUMBO Environmental Chamber. The reflectance signatures in the visible and near IR regions and the BRDF measurements for each sample tested are displayed below. Any small hump in the reflectance spectrum curves present at ~1000 nm is due to the overlap between visible and near infrared detectors receiving data in the spectrometer. The 0° and 90° curves present in all BRDF data plots represent the in-plane and out-of-plane segments where the incident light provided by the MiniDiff optical system is impinging on the surface of the material. Each material sample was analyzed at the 0° and 60° illuminated angle of incidence (AOI).

For weathering experimentation, samples were irradiated throughout each day that measurements were acquired. After the last optical measurement was taken for any given day, the electron gun was turned off and the material samples did not undergo continued irradiation while left in vacuum overnight except for the last night of measurements. Then the electron gun was left on overnight prior to taking the final measurements for both campaigns. Campaign #1 and Campaign #2 samples were irradiated intermittently over a period of 117,180 total seconds and 104,700 total seconds respectively.

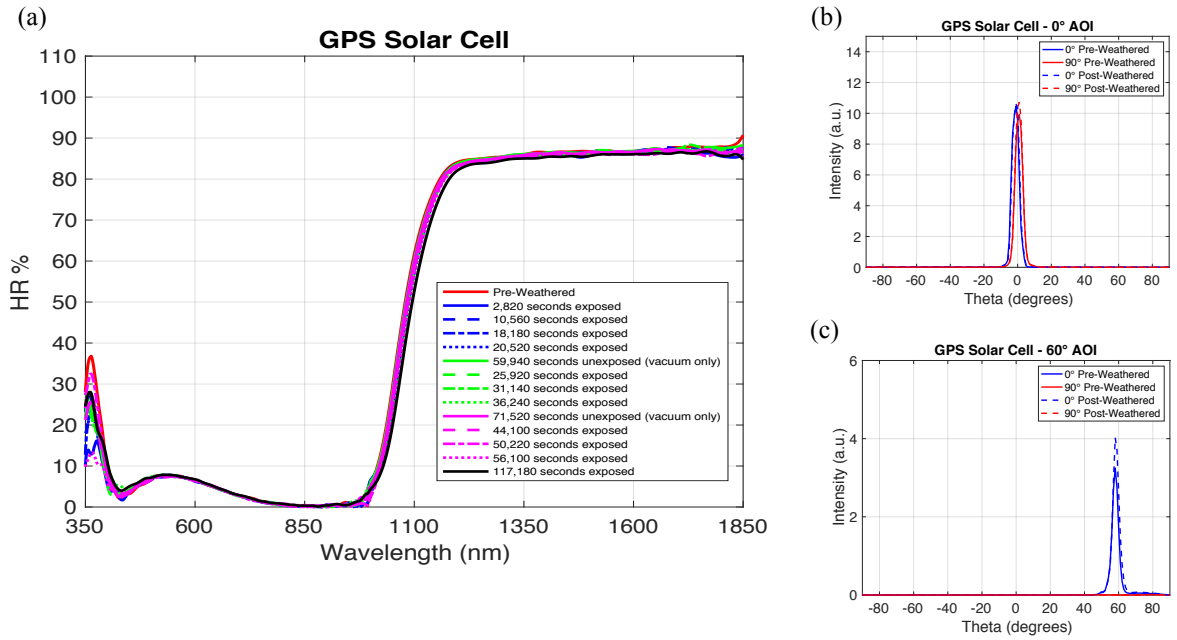

Fig. 2. The (a) reflectance spectrum and BRDF results at (b) 0° and (c) 60° angles of incidence for pre- and post-weathered GPS Solar Cell measured during Campaign #1.

The GPS solar cell produced a spectrum (Fig. 2) indicative of a silicon-based solar cell. This is seen with the low absorption present in the visible region from 350-1000 nm followed by a prominent rise in slope at ~1100 nm. Throughout the 4-day aging process, the solar cell showed great optical stability with little to no changes. This also holds true for the BRDF results, which showed no variation except for the 0° pre- and post-weathered curve. The BRDF at a 60° impingement appeared to increase after having been irradiated.

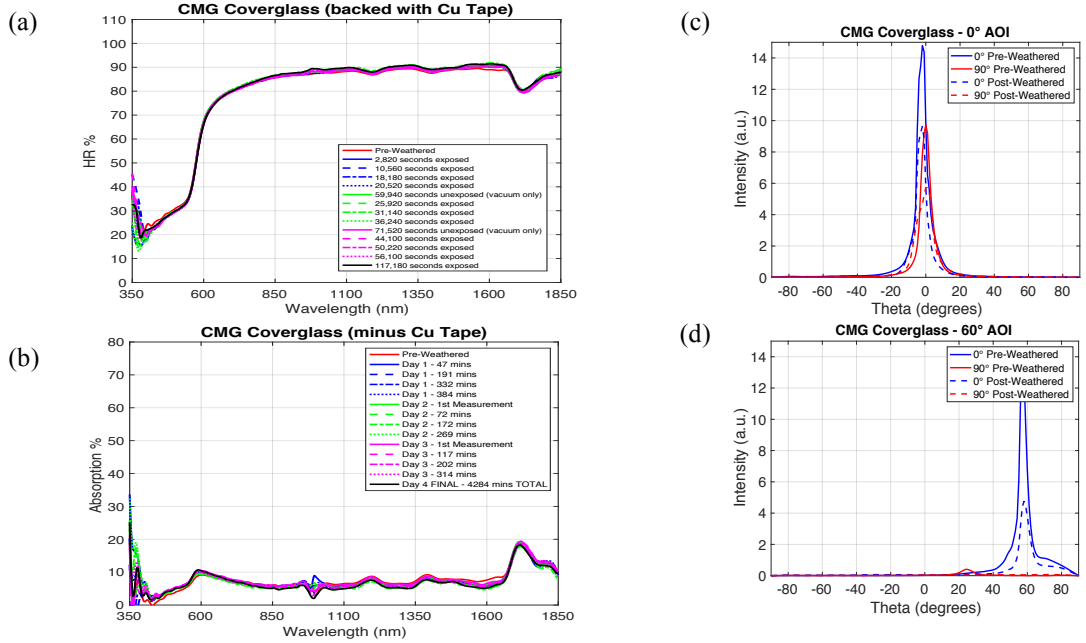

Fig. 3. The (a) reflectance spectrum including and (b) absorption spectrum subtracted from the backed Cu tape and BRDF results at (c) 0° and (d) 60° AOI for pre- and post-weathered CMG cover glass tested during Campaign #1.

The reflectance plots for the CMG, CMO, and CMX cover glass samples produced very similar results, therefore only CMG (Fig. 3a) and CMX (Fig 4a) are displayed in this work. The features seen in their curves most likely are due to the Cu tape used to mount them onto the rotating carousel. This reasoning is drawn from the rise in slope present at ~ 600 nm for all three plots, which is representative of the orange color from the Cu tape (Fig. 5a). This conclusion is considered due to the highly transparent nature of the cover glass. Therefore, to perform analysis on the true spectrum of the CMG and CMO coverglass materials, their reflectance including the Cu tape for mounting was subtracted from the reflectance of the bare Cu tape in its pristine condition (Fig. 3b, Fig. 4b). In doing so it is now apparent that the carbon-hydrogen absorption features present at ~1750 nm (Fig. 3b, Fig. 4b) is a property belonging to the coverglass materials measured since it is absent in the pristine Cu tape spectrum (Fig. 5a). To

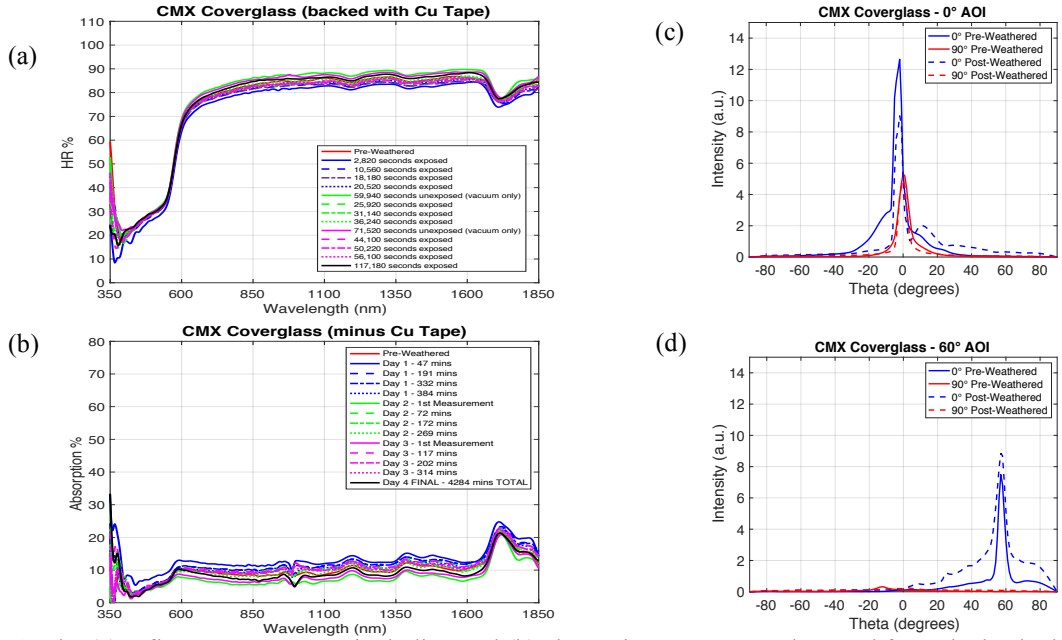

Fig. 4. The (a) reflectance spectrum including and (b) absorption spectrum subtracted from the backed Cu tape and BRDF results at (c) 0° and (d) 60° AOI for pre- and post-weathered CMX cover glass tested during Campaign #1.

enhance the acquisition of this data in the future a 100% reflective mirror surface will be used as a backing material to mount the coverglass onto the sample carousel in the environmental chamber.

The BRDF measurements for all cover glasses resulted in an attenuated response in both 0° and 60° AOI's except for the CMX cover glass measured at a 60° AOI (Fig. 4d). For this incident angle the CMX glass marginally increased in reflectance and appeared slightly more diffuse seen by the broadening of the peak after having been weathered, compared to its decreased response for the 0° AOI.

As seen in the Cu tape backed cover glass reflectance spectra (Fig. 3a, Fig. 4a), the Cu tape depicts a curve with a slope at ~600 nm, which correlated with its physical color property (Fig. 5a). The copper sample's reflectance curve remains mainly flat with a steady increase in slope after ~850 nm which is a common behavior seen in many metals. The pristine Cu tape was used for comparative analysis with the coverglass samples since the electrons bombarding the glasses did not travel through the material deep enough to affect the Cu tape used to mount the coverglasses on the carousel.

The Cu tape produced a highly specular response for its BRDF's for both 0° and 60° AOI and for pre- and post-weathered conditions. Though the signature for the 0° AOI remained close to equal between its pre- and post-weathered result, a large decrease in magnitude can be seen for the 60° AOI (Fig. 5c) and now appears similar to its 0° AOI result.

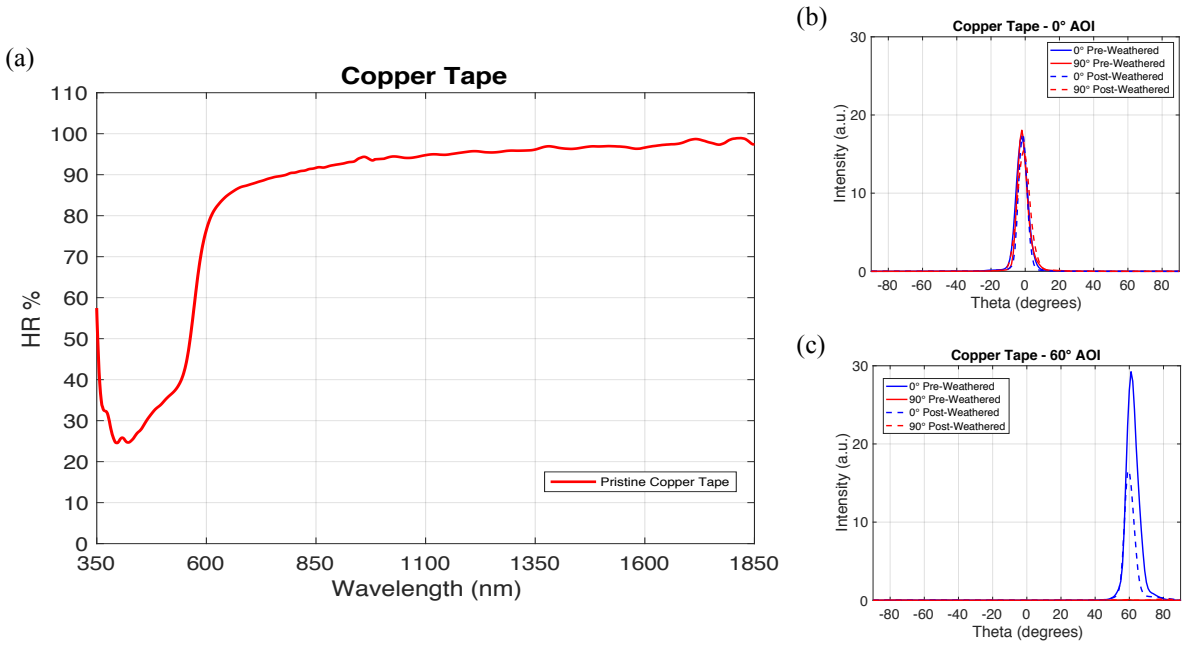

Fig. 5. The (a) pristine reflectance spectrum and BRDF results at (b) 0° and (c) 60° angles of incidence for pre- and post-weathered Cu tape measured during Campaign #1.

The c-c composite provided for this study was dark black in physical appearance, a characteristic that attributed to its extremely low HR percent (Fig. 6a). The material maintained a great deal of absorption throughout its entire spectrum from visible- to near-infrared wavelength regions, almost falling under 0% HR at times, showing that it had comparable absorption to that of the Acktar black material used for calibration purposes. The spectrum results for the c-c composite exhibited great stability throughout the entire measurement campaign save for the final measurement taken on the morning of Day 3, where the spectrum resulted in an overall increase. This is additionally proven in its BRDF measurements taken at 0° AOI, where the post-weathered curves show a higher intensity at the 0° theta peak than the pre-weathered result (Fig. 6b). The c-c composite demonstrated more of a specular response at 0° AOI, versus 60° AOI where there was diffuse scattered light along the topography of the sample seen by the various peaks and hills in its curve from -90° to 90° theta (Fig. 6c).

Black paints RM-550, AZ-1000-ECB, and MLS-85 produced closely identical reflectance spectra to one another, and even to that of the c-c composite. For this reason, only the reflectance and BRDF plots for the RM-550 black paint material sample are presented (Fig. 7). The three black paints' reflectance maintained great absorption throughout the entire plotted wavelength region, so great that the reflectance values fell under 0% when surpassing

1000 nm wavelengths in the near infrared section. This indicates that these black paint materials provide an optical reflectance that is lower than the Acktar black material used for calibration reasons. A reason could be that the Acktar black used during several space weather-simulation experiments had lost some of its pristine material properties. Employing a new Acktar black material for future measurements will likely provide results closer to the true reflectance value of such dark samples. The reflectance of the RM-550, AZ-1000-ECB, and MLS-85 black paints remained consistent throughout the weathering experiment, showing no major increases or decreases in reflection except for the final measurement taken on Day 3, where the reflectance increased similar to what was seen for the c-c composite (Fig. 6a). However, this was not seen in the MLS-85-C black paint sample (Fig. 8a) where its reflectance spectrum was stable, remaining consistent and maintaining its optical properties within the 350-1850 nm wavelength range throughout the entire duration of experimentation.

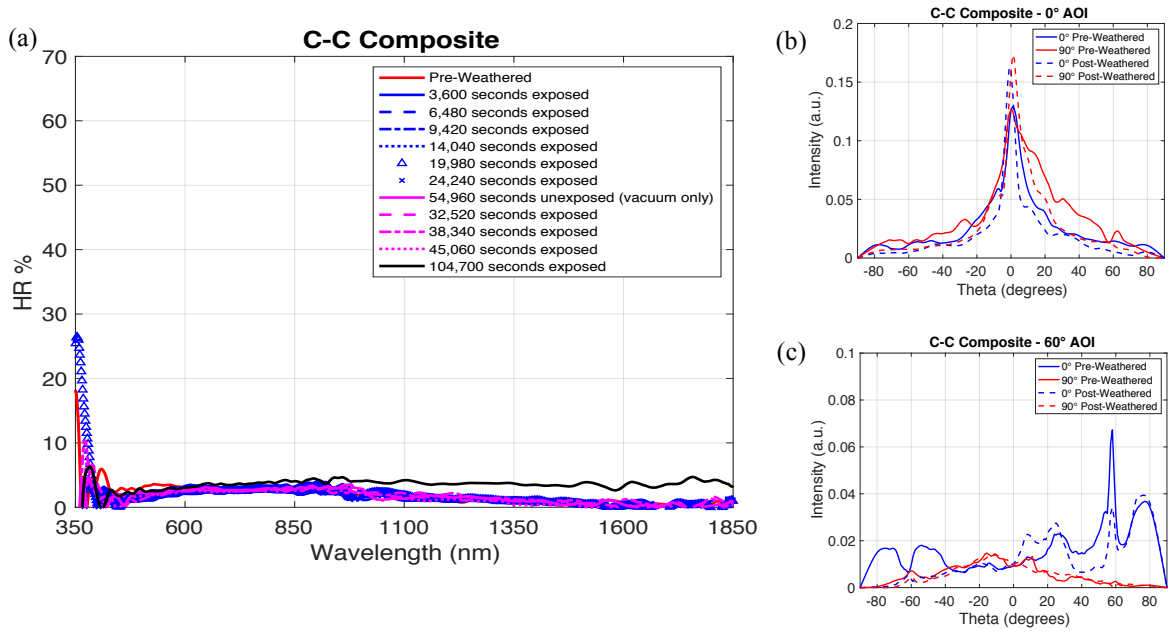

Fig. 6. The (a) reflectance spectrum and BRDF results at (b) 0° and (c) 60° angles of incidence for pre- and post-weathered c-c composite measured during Campaign #2.

All four black paints demonstrated a specular response when impinged at 0° AOI and exhibited diffuse reflectance characteristics at a 60° angle of incidence. They produced a lower BRDF after undergoing electron radiation seen in the post-weathered curves for the 0° AOI, however the RM-550 black paint sample exhibited a smaller amount of decreased intensity (Fig. 7b) than the other paints, which had a much larger decrease in intensity as seen in the MLS-85-C 0° AOI BRDF plot (Fig. 8b). The results for the 60° AOI show the data curves to be relatively similar for pre- and post-weathered outcomes (Fig. 7c and Fig. 8c).

The reflectance results for Kapton produced nearly identical results from testing during both Campaigns #1 and #2. For this reason, only Kapton reflectance data acquired from Campaign #1 are presented in this study. The reflectance curve for the MLI component (Fig. 9a) shows the material's orange color quality in the visible spectrum region at ~600 nm with the increase in slope. There is a slight dip near ~850 nm followed by a continuous steady rise in slope through 1850 nm. These details are commonly seen for Kapton and are well representative of the material. The depression in the curve present at ~1700 nm is often due to carbon-hydrogen bonding in the material's chemical make-up.

The reflectance percent for the Kapton showed continual attenuation during the time that the sample was undergoing radiation exposure from electron bombardment. Throughout the measurement campaign, when the sample was first measured each morning after radiation had been halted for ~15 hours each night, the reflectance spectrum percentage rose to match the spectrum of the material in its pristine condition prior to irradiation, showing a level of recovery in material properties. This is generally seen in polymeric materials and likely occurred because Kapton is a polyimide film. The chemical structure of polymers is affected by high-energy electrons resulting from the breaking of molecular bonds to form radicals, which can then reform into matching bonds present in the pristine polymer, leading to a recovered material spectral curve [4].

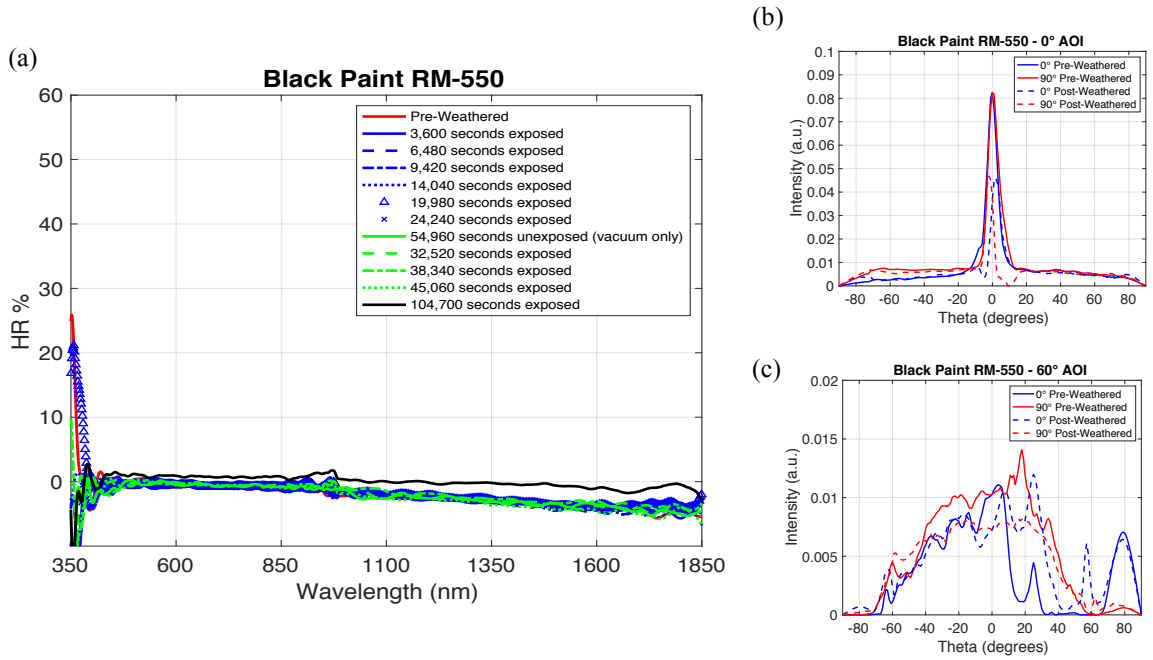

Fig. 7. The (a) reflectance spectrum and BRDF results at (b) 0° and (c) 60° angles of incidence for pre- and post-weathered black paint RM-550 measured during Campaign #2.

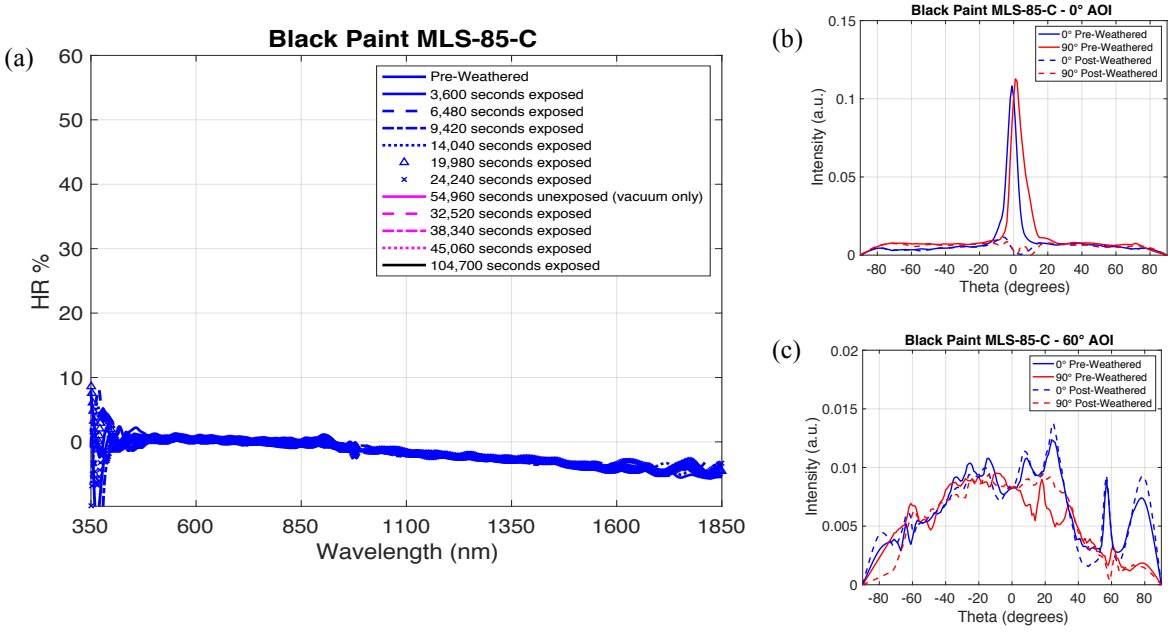

Fig. 8. The (a) reflectance spectrum and BRDF results at (b) 0° and (c) 60° angles of incidence for pre- and post-weathered black paint MLS-85-C measured during Campaign #2.

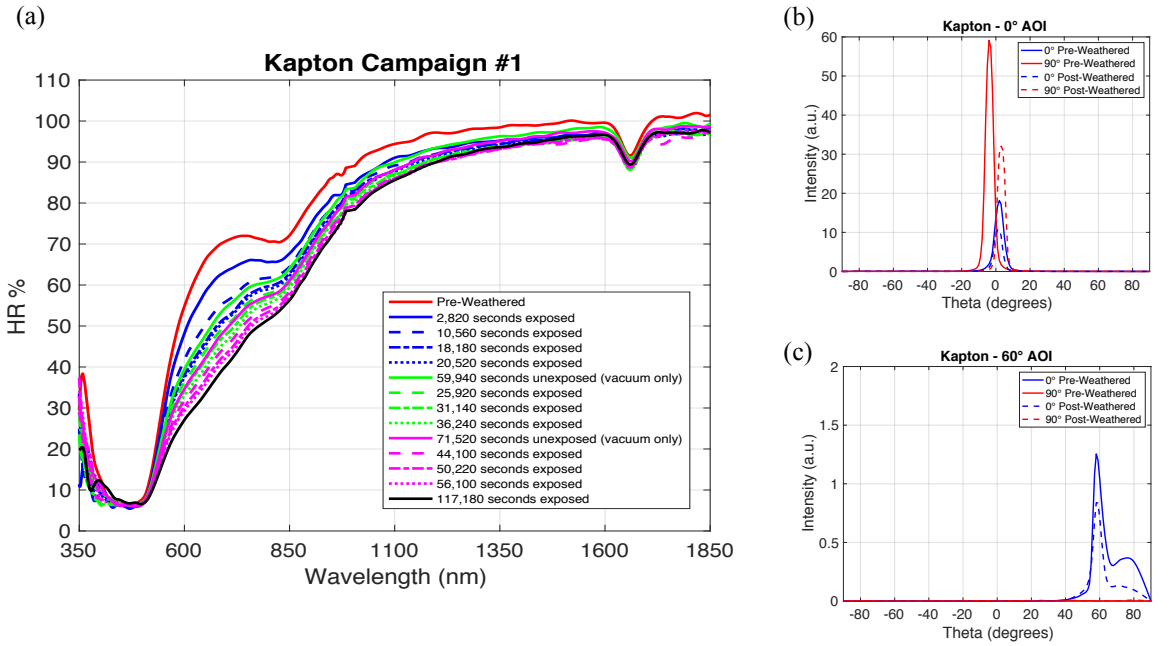

Fig. 9. The (a) reflectance spectrum and BRDF results at (b) 0° and (c) 60° angles of incidence for pre- and post-weathered Kapton measured during Campaign #1.

Kapton samples in Campaigns #1 and #2 resulted in a BRDF magnitude that was much lower after being weathered for both 0° and 60° AOI accounts. It is also to be noted that for the 0° AOI, the polyimide film had a very specular response seen in the sharp peaks of the curves (Fig. 9b). The 60° AOI for the Kapton used in Campaign #1 was still specular though also having some diffuse characteristics, which resulted in the peak broadening out between the 60° and 80° range. The Kapton sample in Campaign #2 produced an entirely specular response for 0° and 60° angles of incidence.

5 SUMMARY

Certain conclusions can be drawn regarding optical property changes for different classifications of materials after being irradiated for given amounts of time. Kapton behaved as expected during both measurement campaigns, showing evident amounts of recovery at foreseeable times of measurement. The CMG, CMO, and CMX cover glasses produced spectrum results comparable to what was seen for the Cu tape, suggesting that these glasses provided high transparency and would thus contribute information regarding the material that sits beneath them. The GPS solar cell and MLS-85-C displayed great optical stability throughout space weather simulations, as did the c-c composite and RM-550, AZ-1000-ECB, and MLS-85 black paints. All four black paints and the c-c composite exhibited a great deal of absorption throughout the visible and near infrared regions of the spectrum as anticipated. BRDF can determine the magnitude of a surface reflection and how it differs depending on the angle of light impinging on it, while reflectance spectroscopy can help characterize materials from their chemistry, physical properties, and optical properties.

6 FUTURE WORK

This experimentation will be applied to achieve a deeper understanding of material optical properties by using a goniometer. This will allow the BRDF of material surfaces to be measured at multiple angles, which will enhance and augment collected data particularly with determination of object position in orbit. The goniometer will be designed to attain BRDF measurements over the 350-2500 nm spectrum, rather than only at the 632 nm wavelength provided by the Mini-Diff system used in this study. Measurements will be performed on a wide variety of materials having different topographical qualities, including selected materials examined in this presented work. Material taxonomy will be performed on the collected BRDF and reflectance data to arrange spectra results into material families. Major material families will include metals, polymers, ceramics, and composites, and major families will be broken down into subsets such as metal alloys versus pure metals, or organics versus inorganics. Material taxonomy will benefit by sampling spectral data from material families instead of only individual samples.

7 REFERENCES

1. Chertok, B., & Siddiqi, A. "*Rockets and People Volume IV: The Moon Race,"* National Aeronautics and Space Administration Office of Communications History Program Office, Washington, DC, 2011.
2. Schildknecht, T. "Advanced Maui Optical and Space Surveillance Technologies Conference," in *Advanced Maui Optical and Space Surveillance Technologies Conference*, 11 Sep 2018.
3. Anz-Meador, P. and Shoots, D., Eds. *Orbital Debris Quarterly News*, Vol. 3, no. 1 & 2, May 2019.
4. Engelhart, D.P., Plis, E.A., D. Ferguson, D., *et al.* "Space Plasma Interactions with Spacecraft Materials," *Plasma Science and Technology - Basic Fundamentals and Modern Applications*, 2019.
5. Reyes, J.A., Miller, B.G., Plis, E.A., *et al.* "Understanding optical changes in on-orbit spacecraft materials," Proc. SPIE 11127, Earth Observing Systems XXIV, 111270I (9 September 2019); https://doi.org/10.1117/12.2528926
6. Bedard, M.D., Levesque, M., and Wallace, B. "Measurement of the photometric and spectral BRDF of small Canadian satellites in a controlled environment," DRDC-VALCARTIER-SL-2011-343, pg. 7, 2011.
7. Hostetler, J. and Cowardin, H. "Experimentally-Derived Bidirectional Reflectance Distribution Function Data in Support of the Orbital Debris Program Office," in *AMOS 2019 Conference Proceedings*, 2019.
8. Reyes, J.A. and Cone, D.A. "Characterization of Spacecraft Materials using Reflectance Spectroscopy," in *AMOS 2019 Conference Proceedings*, 2019.
9. "SR-3501 Portable Spectroradiometer with Expanded Spectral Range," *Spectral Evolution*. [Online]. Available: https://spectralevolution.com/products/hardware/compact-lab-spectroradiometers/sr-3501/. [Accessed: 17 Aug 2019].
10. "Qioptiq Space: Cover glass: Optical solar reflector OSR," Qioptiq Space | Cover glass | Optical solar reflector OSR. [Online]. Available: http://www.qioptiq.com/space.html. [Accessed: 21 Aug 2019].
11. Devi, G.R. and Rao, K.R. "Carbon-Carbon Composites - An Overview," *Defense Science Journal*, Vol. 43, no. 4, pp. 369–383, Oct. 1993.
12. "AZ Technology: Materials, Paint and Coatings," *AZ Technology | Materials, Paint and Coatings*. [Online]. Available: http://www.aztechnology.com/materials-coatings.html. [Accessed: 17 Aug 2019].
13. Engelhart, D.P., Maxwell, J., Bengston, M., *et al.* "Optical degradation and recovery of multilayer insulation in a simulated GEO environment," in *Optical degradation and recovery of multilayer insulation in a simulated GEO environment*, 2018.
14. Bengtson,M., Maxwell, J., Hoffmann, r., *et al.* "Optical Characterization of Commonly Used Thermal Control Paints in a Simulated GEO Environment," in *Optical Characterization of Commonly Used Thermal Control Paints in a Simulated GEO Environment*.
15. "DuPont™ Kapton® 50HN Polyimide Film, 13 Micron Thickness," *MatWeb Material Property Data*. [Online]. Available: http://www.matweb.com/search/DataSheet.aspx?MatGUID=99c680bc28dd409fb7e8fd3ddbcee537&ckck=1. [Accessed: 17-Aug-2019].
16. Reyes, J.A. "Technical Engineering Memorandum," Air Force Research Labs, 2019.